Key Motif to Gain Selectivity at the Neuropeptide Y_5-Receptor: Structure and Dynamics of Micelle-Bound [Ala^{31}, Pro^{32}]-NPY[†,‡]

Reto Bader,[§,||] Gabriela Rytz,[§] Mirjam Lerch,[§] Annette G. Beck-Sickinger,[⊥] and Oliver Zerbe*[,§]

Institute of Pharmaceutical Sciences, ETH Zürich, Winterthurerstrasse 190, 8057 Zürich, Switzerland, and Institute of Biochemistry, University of Leipzig, Talstrasse 33, 04103 Leipzig, Germany

Received February 18, 2002; Revised Manuscript Received April 4, 2002

ABSTRACT: The structure of [Ala^{31}, Pro^{32}]-NPY, a neuropeptide Y mutant with selectivity for the NPY Y_5-receptor (Cabrele, C., Wieland, H. A., Stidsen, C., Beck-Sickinger, A. G., (2002) *Biochemistry XX*, XXXX-XXXX (companion paper)), has been characterized in the presence of the membrane mimetic dodecylphosphocholine (DPC) micelles using high-resolution NMR techniques. The overall topology closely resembles the fold of the previously described Y_5-receptor-selective agonist [Ala^{31}, Aib^{32}]-NPY (Cabrele, C., Langer, M., Bader, R., Wieland, H. A., Doods, H. N., Zerbe, O., and Beck-Sickinger, A. G. (2000) *J. Biol. Chem 275*, 36043−36048). Similar to wild-type neuropeptide Y (NPY) and [Ala^{31}, Aib^{32}]-NPY, the N-terminal residues Tyr^1−Asp^{16} are disordered in solution. Starting from residue Leu^{17}, an α helix extends toward the C-terminus. The decreased density of medium-range NOEs for the C-terminal residues resulting in larger RMSD values for the backbone atoms of Ala^{31}−Tyr^{36} indicates that the α helix has become interrupted through the [Ala^{31}, Pro^{32}] mutation. This finding is further supported by ^{15}N-relaxation data through which we can demonstrate that the well-defined α helix is restricted to residues 17−31, with the C-terminal tetrapeptide displaying increased flexibility as compared to NPY. Surprisingly, increased generalized order parameter as well as decreased $^3J_{HN\alpha}$ scalar coupling constants reveal that the central helix is stabilized in comparison to wild-type NPY. Micelle-integrating spin labels were used to probe the mode of association of the helix with the membrane mimetic. The Y_5-receptor-selective mutant and NPY share a similar orientation, which is parallel to the lipid surface. However, signal reductions due to efficient electron, nuclear spin relaxation were much less pronounced for the surface-averted residues in [Ala^{31}, Pro^{32}]-NPY when compared to wild-type DPC-bound NPY. Only the signals of residues Asn^{29} and Leu^{30} were significantly more reduced in the mutant. The postulation of a different membrane binding mode of [Ala^{31}, Pro^{32}]-NPY is further supported by the faster H/D exchange at the C-terminal amide protons. We conclude that arginine residues 33 and 35, which are believed to be directly involved in forming contacts to acidic receptor residues at the membrane−water interface, are no longer fixed in a well-defined conformation close to the membrane surface in [Ala^{31}, Pro^{32}]-NPY.

Neuropeptide Y (NPY)[1] is a 36-residue C-terminally amidated polypeptide hormone (*2*). At least four Y-receptor subtypes (Y_1, Y_2, Y_4, and Y_5), all belonging to the rhodopsin-like family of G-protein coupled receptors and located in the central or peripheral nervous system (*3*), are activated by NPY (*4*). In the brain, NPY is the most abundant neuropeptide and has been implicated in several regulatory functions (*5*). Injection of NPY directly into the paraventricular nucleus of the hypothalamus of satiated brain-cannulated rats produced a large, dose-dependent increase in food intake (*6*). Especially the possible pharmacological role of hypothalamic NPY for the regulation of food-uptake and hence its influence on obesity has steered a number of pharmacological investigations using peptide analogues, receptor gene-knockout animals, and receptor-specific antagonists. These lead to the suggestion that the Y_1- and Y_5-receptors are important in mediating the effects of NPY on food intake in rats (for a review, see ref *7*). To characterize each of the two potential "feeding receptor subtypes" individually, we focus our efforts on the development of potent and selective agonists and antagonists for the individual receptor subtypes. Selective or partially selective antagonists have been available for both Y_1- and Y_5-receptor subtypes for some time and could be shown to inhibit NPY-

† This work was supported by ETH Zürich Grants Nos. 0 20 439-97 and TH-39/00-3.

‡ The atomic coordinates have been deposited in the Protein Data Bank (entry 1ICY).

* To whom correspondence should be addressed at Institute of Pharmaceutical Sciences, ETH Zürich, Winterthurerstrasse 190, 8057 Zürich, Switzerland. Phone: +41 1 635 60 81. Fax: +41 635 68 84. E-mail: oliver.zerbe@pharma.anbi.ethz.ch.

§ Institute of Pharmaceutical Sciences, ETH Zürich.

|| Present address: Department of Chemistry, University of Cambridge, Lensfield Road, Cambridge CB2 1EW, U.K.

⊥ University of Leipzig.

[1] Abbreviations: Aib, aminoisobutyric acid; doxyl, 4,4-dimethyl-3-oxazolidinyloxy; CD, circular dichroism; DPC, dodecylphosphocholine; G-protein, guanine-nucleotide-binding regulatory protein; HSQC, heteronuclear single-quantum spectroscopy; Hyp, hydroxyproline; NOE, nuclear Overhauser enhancement; NOESY, nuclear Overhauser enhancement spectroscopy; NPY, neuropeptide Y (p = porcine); PP, pancreatic polypeptide; R_1, longitudinal relaxation rate constant; R_2, transverse relaxation rate constant; RMSD, root-mean-square deviation; TOCSY, total correlation spectroscopy; TPPI, time proportional phase incrementation.

10.1021/bi0201419 CCC: $22.00
Published on Web 05/25/2002

induced food intake (*8*−*11*). However, we recently presented the first selective agonists at the Y_5-receptor, which indeed turned out to stimulate food intake in rats (*1*). A series of NPY mutants and chimeras of NPY and pancreatic polypeptide (PP), another hormone of high sequence homology to NPY which is targeting similar receptors, were designed and proven to be Y_5-receptor-selective as long as they contained the [Ala[31], Xxx[32]] motif (Cabrele et al., companion paper). Mutants in which Thr[32] was replaced by Aib, Pro, or Hyp bound selectively to the Y_5-receptor with lowered but still good affinity (in the sub-μM range with the [Ala[31], Aib[32]] mutant displaying 10-fold better binding than the corresponding Ala, Pro mutant), whereas the introduction of D-proline lead to a drastic loss of affinity.

In an attempt to understand the spatial properties required for Y_5-receptor selectivity, we previously determined the solution structure of [Ala[31], Aib[32]]-NPY (*1*). The solution structure of wild-type NPY itself has been described in the literature both by Darbon et al. (*12*) and by Monks et al. (*13*). Both publications agree that only the C-terminal part of NPY forms a stable α helix, whereas the N-terminus is much more disordered. However, Darbon et al. propose a polyproline II helix for the N-terminal part that bends back onto the C-terminal helix. This structural feature was described in the crystal structure of avian polypeptide (aPP) by Blundell et al. (*14*) for the first time and hence became known as the PP fold. In contrast, Monks postulates that the N-terminus is fully flexible. We recently have supported the latter view based upon arguments from ^{15}N-relaxation data (*15*). Comparison of the conformation of [Ala[31], Aib[32]]-NPY to that of wild-type NPY revealed a significant change in the C-terminal part of the peptide, which is known to be a key interaction site at all known Y-receptors (*16*, *17*). On the basis of NOE-derived distance restraints, it was found that the mutant adopts a 3_{10}-helical turn between residues 28 and 31, followed by a flexible C-terminus. This is in contrast to the solution structure of NPY by Monks in which a regular α helix extends to the C-terminal end. On the other hand, recent studies of the dynamics of NPY in aqueous solution clearly demonstrated increased flexibility of N−H bond vectors in the C-terminal tetrapeptide as compared to those within the central part of the helix (between residues 16−32) (*15*).

When a pathway that requires a membrane-association step prior to receptor binding is assumed (*18*−*20*), it was suggested that the determination of the structure of the hormones in the presence of a membrane mimetic gives biologically relevant insight into the peptide conformation which is encountered by the receptor during the initial contact. We used micelles formed by the zwitterionic dodecylphosphocholine (DPC) to model the membrane. DPC is the detergent that presents the predominant constituent of animal cell membranes (*21*). It has been designed especially for solution NMR purposes (*22*) and is assumed to give structural results that are in agreement with those obtained using bilayers, at least in the case of surface-associated polypeptides (*23*). As described by Opella et al. (*24*), using a high excess of detergent well above the critical micelle concentration prevents the formation of different states of aggregates. This yields rather well-resolved spectra, whose signal dispersion is even increased due to the polar and charged headgroups.

During our investigations on NPY bound to DPC micelles, we noticed that the C-terminal conformation was slightly rearranged (as compared to the solution structure) so that Tyr[36] is placed close to the membrane−water interface. Moreover, the α helix became significantly stabilized as evident from generalized order parameters larger than 0.8 for residues Ala[18]−Arg[33]. The membrane-anchoring residues were identified by experiments utilizing micelle-integrating spin-labels such as 5- or 12-doxylstearate. In 5-doxylstearate, a paramagnetic label is placed in vicinity of the polar headgroups (*25*); hence, all resonances closer than about 10−20 Å to the spin-label are significantly broadened through efficient spin−electron relaxation (*26*). Thereby, we discovered that NPY is anchored to the membrane through interaction of the phospholipids with the long and hydrophobic/aromatic side-chains of residues of the C-terminal helix.

Here, we examine the structure and dynamics of [Ala[31], Pro[32]]-NPY bound to DPC micelles by ^{1}H NMR and analysis of ^{15}N-relaxation data. We have chosen that particular peptide because it contains solely proteinogenic amino acids and hence can be produced recombinantly required for ^{15}N labeling. The results are compared with the solution structure of [Ala[31], Aib[32]]-NPY and wild-type NPY. We find that Y_5-receptor-selectivity is most probably related to the destabilization of the α-helical conformation at the C-terminal tetrapeptide, as shown for [Ala[31], Aib[32]]-NPY in aqueous solution as well as for [Ala[31], Pro[32]]-NPY bound to DPC micelles. The C-terminus of [Ala[31], Pro[32]]-NPY adopts a large and flexible loop that is differently anchored to the membrane by residues 30 and 36. In contrast, in native NPY, a regular α-helical turn is found, which is anchored by residues 32 and 36. The implications of these findings for a possible alternative binding mode at the Y_5-receptor are discussed.

EXPERIMENTAL PROCEDURES

Materials. $^{15}NH_4Cl$ was purchased from Martek (Columbia, MD), deuterated DPC-d_{38} (99%-*d*), and methanol-d_3 were ordered from Cambridge Isotope Laboratories (Andover, MA). 5-Doxylstearic acid was bought from Aldrich (Buchs, Switzerland). Isotopically nonenriched DPC was obtained from Avanti Polar Lipids (Alabaster, AL). Oligonucleotide primers were synthesized by Microsynth GmbH (Balgach, Switzerland).

Peptide Synthesis. Isotopically nonenriched peptide [Ala[31], Pro[32]]-pNPY was prepared by solid-phase peptide synthesis using 9-fluorenylmethoxycarbonyl (Fmoc) protection group strategy on a robot system (Syro, MultiSynTech, Bochum), as described (Cabrele et al., companion paper). To obtain the peptide amide, 4-(2′,4′-dimethoxyphenyl-Fmoc-aminomethyl)phenoxy resin was used as polymeric support (Novabiochem, Läufelingen, Switzerland). The purity and the molecular weight were checked by reversed-phase high-performance liquid chromatography (HPLC) (column C-18, 3 × 125 mm, 5 mm, flow 0.6 mL/min, gradient 20% acetonitrile to 70% acetonitrile in water/trifluoroacetic acid (100:0.1) within 30 min) and electron spray ionization-mass spectrometry (ESI-MS) (SSQ710, Finnigan, San Jose, CA), respectively.

Cloning, Expression, and Purification of Uniformly ^{15}N-Enriched [Ala[31], Pro[32]]-pNPY. Starting from the plasmid

pUBK19/NPY-G (*15*) that contains the pNPY-Gly DNA fused to the nucleotide sequence of N-terminally decahistidine-tagged yeast ubiquitin (Ub) (*27*), the double mutations I31A/T32P were introduced by site-directed mutagenesis using the QuikChange Mutagenesis Kit (Stratagene, La Jolla, CA). The two complementary primers required in this method (*28*) were chosen as follows: (forward) 5′-CGCTGCGTCACTACATCAACCTGGCTCCGCGTCAGCGTTACGGGTGATAGTCG-3′ and (reverse) 5′-CGACTATCACCCGTAACGCTGACGCGGAGCCAGGTTGATGTAGTGACGCAGCG-3′. For the selection of DNA bearing the mutation, methylated and hemimethylated DNA was digested with *Dpn*I (New England Biolabs, BioConcept, Allschwil, Switzerland) and subsequently transformed into *Escherichia coli* XL2-Blue strain (Stratagene, Amsterdam, The Netherlands). The sequence of the resultant plasmid pUBK19/{AP}-NPY-G was confirmed using dideoxy sequencing.

Expression of uniformly ^{15}N-labeled H_{10}-Ub-[Ala^{31}, Pro^{32}]-NPY-G was performed in the *E. coli* BL21 (DE3) strain on M9 minimal medium with $^{15}NH_4Cl$ as the sole nitrogen source, as described previously (*15*). Isolation under denaturing conditions (6 M guanidine hydrochloride, 50 mM Tris (pH 8.0), 100 mM NaCl, and 1 mM β-mercaptoethanol), purification (using Ni^{2+} affinity chromatography including on-column refolding by continuously decreasing the guanidine concentration of the refolding buffer from 6 to 0 M), and cleavage of the fusion protein by use of ubiquitin hydrolase was done according to the protocol by Kohno et al. (*27*). The separation of [Ala^{31}, Pro^{32}]-NPY-G from H_{10}-Ub was achieved on a Ni^{2+}-NTA-agarose column (Qiagen, Basel, Switzerland) followed by desalting of the eluate using Sep-Pak Plus C_{18} cartridges (10% acetonitrile to 50% acetonitrile in 0.1% trifluoroacetic acid in steps of 10%/10 mL each). The C-terminal α-amidation of [Ala^{31}, Pro^{32}]-NPY-G using peptidylglycine α-amidating enzyme (EC 1.14.17.3; Unigene Laboratories, Fairfield, NJ) was performed as described previously (*15*). Completeness of the reaction was checked by ESI-MS upon reversed-phase C_{18} chromatography purification.

CD Spectroscopy. CD spectra were recorded on a JASCO J-720 spectropolarimeter over the range of 180−250 nm at 37 °C using a water-jacketed 5-mm sample cell. The peptide concentration was 50 μM in the presence of 10 mM DPC in water at pH 6.0. The response time was set to 2 s at a scan speed of 20 nm/min. The sensitivity range was at 10 mdeg, the step resolution at 0.2 nm, and the bandwidth at 2 nm. The background spectrum due to the detergent was subtracted from the spectra of the peptide-containing solutions. High-frequency noise was reduced by application of a low-path Fourier transform filter. Each measurement was performed 4 times. The ellipticity is expressed as mean residue molar ellipticity $[\Theta]_R$ in deg cm^2 dmol^{-1}. The helix content was estimated according to the method of Chen et al. (*29*).

NMR Spectroscopy. The NMR spectra used for the assignment of proton chemical shifts and derivation of distance and dihedral angle restraints were measured using samples containing 2.5 mM [Ala^{31}, Pro^{32}]-pNPY, 300 mM dodecylphosphocholine-d_{38} in either 10% D_2O/90% H_2O or 99% D_2O at pH 6.0 (uncorrected pH meter reading), and 37 °C on a Bruker Avance 600 MHz spectrometer. For measurements of ^{15}N-relaxation data, uniformly ^{15}N-enriched (>99%) [Ala^{31}, Pro^{32}]-pNPY was used at a concentration of 1.0 mM in the presence of 300 mM DPC-d_{38} in 10% D_2O/90% H_2O at 37 °C. The pH was adjusted to 6.0, and data were recorded on both a Bruker Avance 500 and a Bruker Avance 600 instruments operating at nitrogen frequencies of 50.68 and 60.81 MHz, respectively. Proton chemical shifts were referenced relative to the water line ($\delta(H_2O) = 4.63$ ppm at 310 K), and nitrogen shifts were referenced indirectly to liquid NH_3 (*30*). The spectra were processed using the Bruker XWINNMR-2.1 software and transferred into the XEASY (*31*) program. Peak volumes were integrated within the program SPSCAN that uses line shape-deconvolution of signals for proper integration of partially overlapping peaks.

For the identification of the amino acid spin systems, a clean TOCSY (*32*) experiment with a mixing time of 12 ms utilizing continuous-wave presaturation of the water resonance was recorded. NOESY experiments (*33*, *34*), incorporating a filter scheme for zero-quantum suppression (*35*) with a mixing time of 75 ms, were used for both the sequence-specific sequential resonance assignment and the determination of upper proton, proton distance limits required for the structure calculation. Water suppression was obtained using the WATERGATE sequence (*36*). Scalar $^3J_{HN\alpha}$ coupling constants were derived from inverse Fourier transformation of in-phase NOESY peaks involving H^N protons (*37*).

The assignment of nitrogen frequencies and relaxation experiments were derived from [^{15}N,^{1}H]-HSQC (*38*) experiments utilizing the sensitivity enhancement element (*39*, *40*) and water-flip back methodology (*41*). The assignment of the proton, nitrogen correlation maps was significantly supported by information from a 150 ms NOE-relayed [^{15}N,^{1}H]-HSQC experiment.

Relaxation measurements were performed as described (*15*). In essence, proton-detected versions of Carr−Purcell−Meiboom−Gill (R_2), inversion−recovery (R_1), and steady-state ^{15}N{^{1}H} heteronuclear Overhauser effect sequences were used. Water suppression in all of these experiments was achieved through the application of pulsed-field gradients in coherence-selection schemes. For R_1 and R_2 experiments recycle delays of 2.2 s and for the ^{15}N{^{1}H}-NOE delays of 3.2 s were applied. For R_1 (R_2) experiments, 16 (32) scans were accumulated for each increment and 64 scans for each increment in the ^{15}N{^{1}H}-NOE. The R_1 series used the following relaxation delays: 0.03, 0.12, 0.21, 0.76, 1.23, 1.99, and 3.00 s. The R_2 series was run with the following delay settings: 0.004, 0.012, 0.02, 0.04, 0.1, 0.2, 0.4, and 0.6 s. Buildup of the NOE was achieved through a pulse train of 120 degree proton pulses separated by 5 ms over a period of 3 s.

Spin-Label Experiment. The orientation of [Ala^{31}, Pro^{32}]-NPY with respect to the membrane surface was determined by measuring the effect of the micelle-integrating 5-doxyl-stearic acid on relaxation of the backbone $^1H^N$ and $^{15}N^{HN}$ signals through distance-dependent electron, or nuclear-spin relaxation as observed in a [^{15}N,^{1}H]- HSQC spectrum. The methodology has been described for wild-type pNPY in Bader et al. (*15*). The intensities of the cross-peaks before and after addition of the spin-label were determined and compared.

Hydrogen Exchange. For the measurement of proton/deuterium exchange of the amide protons, a protonated ^{15}N-[Ala^{31}, Pro^{32}]-NPY sample was dissolved in D_2O, and 2D

[^{15}N,^{1}H]-HSQC spectra were recorded at different time intervals. Thereby, the disappearance of the ^{15}NH was monitored 10, 40, and 70 min, respectively, upon addition of the solvent.

Structure Calculation. The structure calculation was performed by restrained molecular dynamics in torsion angle space using a simulated annealing protocol as implemented in the program DYANA (*42*), similar to the procedure described previously for pNPY (*15*). From a total of 622 unambiguously assigned NOE cross-peaks and 26 $^{3}J_{HN\alpha}$ coupling constants (of which only those 16 were included that were indicative of nonrotationally averaged torsion angles; i.e., <6 Hz), 207 meaningful upper distance limits, as well as 145 ϕ, ψ, χ^1, and χ^2 torsion angle restraints, were derived. In no case it was possible to obtain stereospecific assignments. The final DYANA calculation was performed with 100 randomized starting structures, and the 30 DYANA conformers with the lowest target function were further refined using the AMBER (*43*) force-field as implemented in the program OPAL (*44*). The quality of the final 17 energy-minimized conformers with NMR energies less than 3 kcal/mol was checked in the range of residues 17−29 using the program PROCHECK-NMR (*45*). The figures were prepared with the program MOLMOL (*46*). The NMR ensemble of 17 energy-minimized conformers has been deposited in the Research Collaboratory for Structural Bioinformatics PDB code 1ICY.

Relaxation Data Analysis. Relaxation rate constants R_1, R_2, and NOE enhancements including their associated uncertainties were determined as previously described for wild-type pNPY (*15*). The parameters were interpreted by application of the modelfree-approach (*47*−*49*) using the Modelfree (version 4.01) software package (*50*, *51*). We followed the previously described protocols for estimation of the initial overall rotational correlation time, selection of model-free parameters for adequate description of the experimental relaxation data, and optimization of the motional parameters (*15*). The statistical approach suggested by Mandel et al. (*51*) was applied, and the following models were used in the fitting procedure: (1) S^2; (2) S^2, τ_e; (3) S^2, R_{ex}; (4) S^2, τ_e, R_{ex}; (5) S_f^2, S_s^2, τ_e. Experimental errors for R_1 and R_2 at both applied fields were approximately 3% as determined from duplicated measurements. For large negative values of the ^{15}N{^{1}H}-NOE saturation−transfer mediated effects due to more elevated water−amide proton exchange at pH = 6 lead to largely erroneous values of the heteronuclear NOE; hence, the data for residues 4, 6, and 7 were excluded from the analysis. Otherwise, the error was calculated from estimates of the baseplane noise in the spectra and set to approximately 10% or at minimum 0.1 for NOE values between −1 and +1.

RESULTS

We have defined the experimental conditions for the determination of the structure and dynamics of [Ala^{31}, Pro^{32}]-NPY highly similarly to those described for wild-type pNPY (*15*), thereby allowing a direct comparison of the data. In doing so, diagnostic structural properties of [Ala^{31}, Pro^{32}]-NPY that might be typical for selectivity at the Y_5-receptor can possibly be identified.

In the presence of 300 mM DPC at pH 6.0, wild-type pNPY is monomeric and bound to the micelles. However, despite the elevated pH, only the amide protons of the first three N-terminal residues were significantly affected by exchange broadening. Moreover, the α helix became stabilized, and the signal dispersion was increased due to the presence of polar and charged headgroups. For many peptide hormones such as opioids and neurokinins (*20*, *52*), parathyroid hormone (*53*), and cholecystokinin (*18*, *54*), a pathway for receptor binding that includes membrane association as an initial step has been proposed. We therefore felt encouraged to conduct our studies in a membrane-mimicking environment.

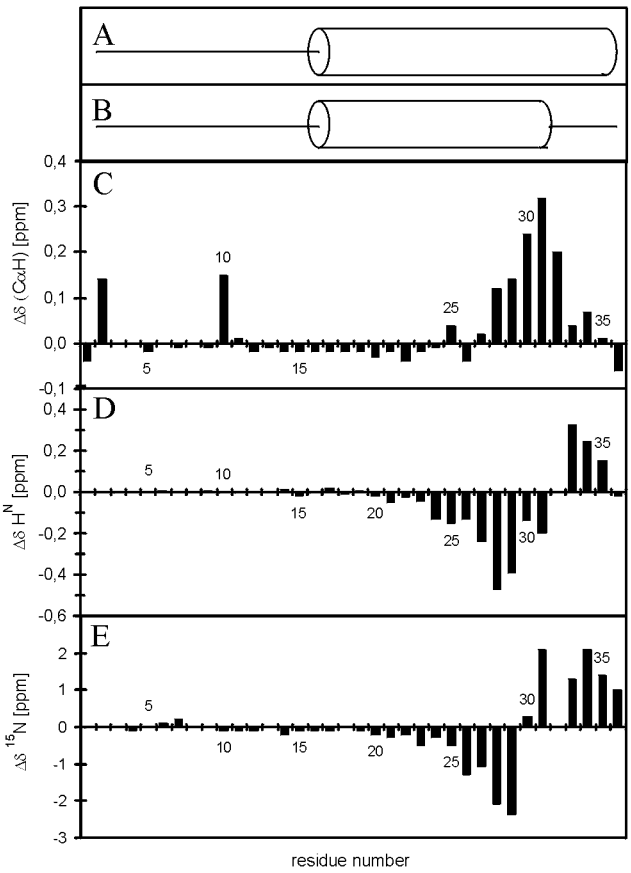

FIGURE 1: (A) Secondary structure of wild-type NPY on DPC micelles according to Bader et al. (*15*). (B) Secondary structure of [Ala^{31}, Pro^{32}]-NPY on DPC micelles (this work). (C) Secondary chemical shift differences for the C_αH, (D) for the H^N, and (E) for the ^{15}N resonance between [Ala^{31}, Pro^{32}]-NPY and NPY bound to DPC micelles. The secondary chemical shift deviations of the C_αH, the H^N protons, and ^{15}N of NPY, respectively, were subtracted from the corresponding values of [Ala^{31}, Pro^{32}]-NPY. Sequence-corrected values were used for the calculation of the ^{15}N secondary chemical shift deviations (*76*).

The chemical shifts of the proton resonances were assigned according to standard methodology (*55*). The assignments for the N-terminal residues Tyr^1−Arg^{19} were supported by the fact that they were nearly perfectly identical to the values found for NPY on DPC micelles (*15*). The residue-specific nitrogen frequencies could subsequently be determined using [^{15}N,^{1}H]-HSQC and NOE-relayed [^{15}N,^{1}H]-HSQC correlation maps. Again, the resonances of residues Tyr^1−Arg^{19} were very similar in both peptides (Figure 1 CDE).

Secondary Chemical Shifts. Wishart et al. (*56*) found a strong relationship between chemical shifts and the protein conformation, and the chemical shift index (CSI) introduced by them has been recognized as a simple and rapid method

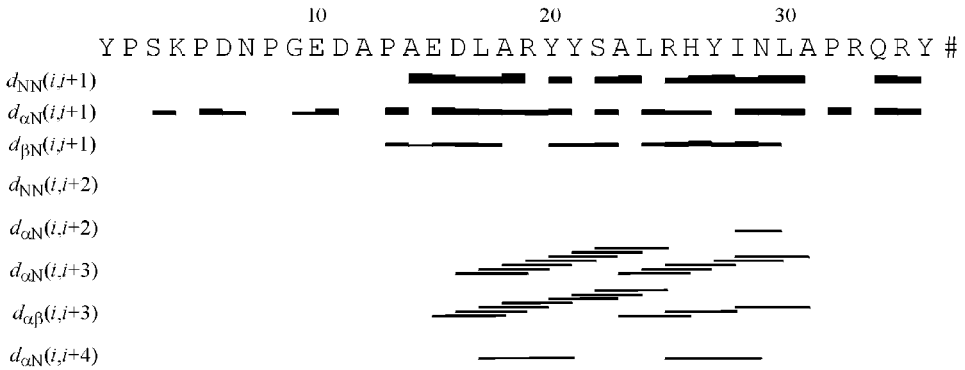

FIGURE 2: Summary of the meaningful distances as derived from the interresidual NOEs between the backbone H^N, H^α, and H^β of [Ala^{31}, Pro^{32}]-NPY on DPC micelles.

to assign secondary structure elements solely based on the analysis of the chemical shifts. For proteins in a α-helical conformation, it was discovered that the ^{1}H NMR chemical shift of the $C_\alpha H$ proton of all 20 naturally occurring amino acids experience a mean upfield shift of 0.39 ppm with respect to the values encountered in disordered (random coil) conformations. This relationship, which was originally based on empirical (statistical) data, could later on be theoretically validated by ab initio quantum-mechanical calculations of H^N and ^{15}N chemical shifts (*57*). For ^{15}N nuclei, major factors determining the chemical shift are χ^1 side-chain conformations, direct (and to a lesser amount indirect) effects due to hydrogen bonding, as well as the electrostatic field of the protein. According to the CSI protocol of Wishart et al. (*58*), [Ala^{31}, Pro^{32}]-NPY is uniquely folded into a α-helical conformation between residues Asp^{16}−Ala^{31} (Figure 1 B) (for a complete listing of the proton chemical shifts and their deviations from the corresponding random coil values (the so-called secondary chemical shifts) see the Supporting Information), a finding which is clearly confirmed by NOE and supported by ^{15}N-relaxation data ($S^2 > 0.5$) (see the following discussion).

The following is based upon a comparison of secondary chemical shifts of $C_\alpha H$ and from H^N and ^{15}N resonances as derived from the Y_5-receptor-selective mutant [Ala^{31}, Pro^{32}]-NPY and from wild-type NPY. (1) We recognize that consecutive downfield differences in the secondary chemical shifts of the $C_\alpha H$ proton larger than 0.1 ppm are observed only in the segment Asn^{29}−Arg^{33}, indicating a local perturbation/destabilization of the secondary structure with respect to the α helix which is normally found in wild-type NPY at this segment (Figure 1 C). (2) We noticed downfield secondary chemical shifts for the amide protons of [Ala^{31}, Pro^{32}]-NPY on the hydrophobic side following a periodic pattern. A similar pattern was discovered for pNPY bound to DPC micelles (*15*) and was interpreted to indicate interactions of the phospholipid headgroups with the amide protons or weaker intramolecular hydrogen bonding of the lipid-exposed backbone amide protons (*56*, *59*). Moreover, it has been reported in the literature that secondary chemical shifts of amide protons in α-helical conformations are often found to be periodic in amphiphilic helices (*60*). (3) Interestingly, when directly comparing the resonance positions of [Ala^{31}, Pro^{32}]-NPY with wild-type NPY, increasing upfield secondary chemical shift differences are found for both the H^N and the corresponding ^{15}N resonances in the region of Tyr^{21}−Asn^{29} (Figure 1, parts D and E). We contribute this effect to a stabilization of the α helix in that segment of the polypeptide chain. This stabilizing effect is also evident from the scalar $^3J_{HN\alpha}$ couplings and the generalized order parameters S^2 (vide infra). The decrease of the absolute value for residues Leu^{30} and Ala^{31} most likely reflects an indirect effect (*57*) due to the loss of hydrogen bonds of the corresponding carbonyl oxygens to amide protons from residues further down the sequence. (*4*) Pronounced downfield secondary chemical shift differences are found at Arg^{33}/Gln^{34} for both H^N and ^{15}N resonances, which is attributed to increased flexibility at the C-terminus of the mutant. It may also be due to an increased distance to the charged headgroups of the phospholipids. Again, this finding is further supported by coupling constants and relaxation data (see the following discussion).

Interresidual NOEs and Coupling Constants. Except for unresolved cross-peaks between the residue pairs 19/20, 21/22, and 24/25 all of the possible H_i^N/H_{i+1}^N, sequential NOEs were observed in the segment 14−31, which is indicative for a well-structured peptide in helical conformation (*55*). In full agreement with this suggestion, many H_i^α/H_{i+3}^N and H_i^α/H_{i+3}^β NOE connectivities are present throughout this region (Figure 2). Interestingly, both types of (i,i+3) NOE cross-peaks are missing between residues 26 and 29, replaced by an H_{25}^α/H_{29}^N NOE. On the contrary, an H_i^α/H_{i+2}^N NOE is found between residues 29 and 31. This is compatible with the view that the two subsequent α-helical turns as found in wild-type NPY are modified to form a wider turn between residues 25 and 29 and a more narrow one between 28 and 31 in the mutant, possibly due to different side-chain/membrane interactions (see the following discussion). Any medium-range NOEs are completely lacking at the C-terminal pentapeptide, suggesting this segment to be in a more extended rather than helical conformation.

Figure 3 shows the CD spectra of NPY and the mutant each of them on DPC micelles at pH 6.0 and 37 °C. Both curves indicate a maximum at 192 nm and a minimum at 209 nm. A second local minimum at 220 nm indicating the presence of α-helical conformation, is clearly less intense in the mutant compared to wild-type NPY. Again, this demonstrates the reduction of helicity upon substitution of Ile^{31}−Thr^{32} by Ala-Pro and supports the results obtained for another Y_5-receptor-selective mutant, [Ala^{31}, Aib^{32}]-NPY, studied in aqueous solution (*1*).

A major difference between NPY and [Ala^{31}, Pro^{32}]-NPY concerns the values adopted by the vicinal $^3J_{HN\alpha}$ coupling constants of residues 16−28, all of which are in the range

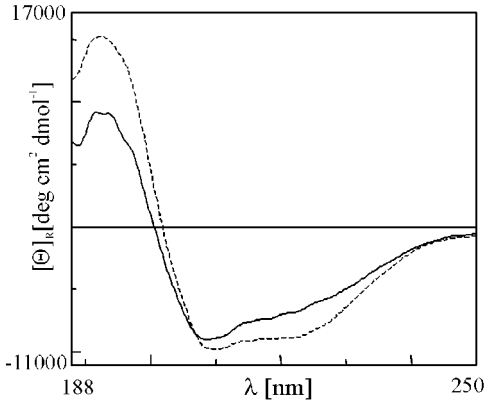

FIGURE 3: CD spectra of 50 μM [Ala^{31}, Pro^{32}]-NPY (—) and NPY (- - -) in the presence of 10 mM DPC micelles.

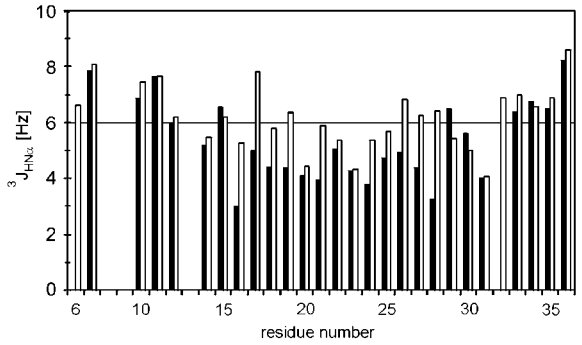

FIGURE 4: Comparison of the vicinal $^3J_{HN\alpha}$ coupling constants between [Ala^{31}, Pro^{32}]-NPY (black bars) and wild-type NPY (white bars) bound to DPC micelles.

of 3−5 Hz and correspond to ϕ-angles similar to those found in stable α helices (*61*, *62*). Most of them are significantly higher in wild-type NPY, some even around 6 Hz (*15*). This gives evidence for a rigidified backbone conformation of residues 16−28 in the Y_5-receptor-selective mutant. Values >6 Hz for the N-terminal residues as well as for the C-terminal tetrapeptide are similar in NPY and the mutant, and they indicate rotationally averaged ϕ-angles usually encountered in more flexible segments (Figure 4).

Three-Dimensional Structure. Some 30 low-energy three-dimensional structures were generated using a total of 67 intraresidual, 67 sequential, and 73 medium-range ($i-j$ = 2, 3, 4) meaningful upper-limit distance restraints and 145 dihedral angle restraints. The structures were calculated with molecular dynamics in torsion angle space using a simulated annealing protocol as implemented in the program DYANA (*42*), followed by an energy minimization with the AMBER (*43*) force field. The 17 lowest NMR-energy term structures out of this set were further surveyed. They contained no distance violations larger than 0.15 Å. Statistical information on the structure calculation is provided in the Supporting Information. The residue-specific atomic root-mean-square deviation (RMSD) for the backbone heavy atoms decreased from 26.7 at Tyr^1 to 1.3 at Asp^{16} and was <1.0 in the region between Leu^{17} and Leu^{30}. At the C-terminus, it increased to 12.7 at Tyr^{36}. All of the structures were α-helical in the segment between Asp^{16} and Leu^{30} (Figure 5).

Best convergence of the resulting structures was observed for the region between Tyr^{21} and Asn^{29} with a RMSD of 0.26 (±0.10) Å for the backbone heavy atoms and 1.35 (±0.37) Å for all heavy atoms, respectively. In most of the

FIGURE 5: Backbone atoms (C_α, N, and C) of 17 minimized structures for [Ala^{31}, Pro^{32}]-NPY on DPC micelles, superimposed over the backbone atoms of residues Tyr^{21}-Asn^{29}.

structures, nearly all residues between Glu^{15} and Leu^{30} were involved in either (i,i+4) or (i,i+3) hydrogen bonds. Hence, the results from the tertiary structure calculation supported the suggestions based upon NOE pattern and chemical shift analysis. These findings are in accordance with the results from NMR relaxation measurements that showed a highly flexible N-terminus, a stable helical segment consisting of residues Leu^{17} to Leu^{30}, and a decrease in stability at the C-terminus. The nearly complete lack of NOEs in the C-terminal pentapeptide results in a highly disordered C-terminus. However, as shown by spin-label experiments (see the following discussion), the Tyr^{36} amide comes into proximity of the membrane and can therefore be considered as being restrained to 2D diffusion on the micelle surface, rather than randomly diffusing in 3D space.

Topological Orientation. The membrane-integrating 5-doxylstearic acid was added at a concentration of approximately 1 spin-label/micelle. The doxyl group that contains an unpaired electron becomes located in the vicinity of the headgroups at the micelle surface (*25*) and thereby leads to significantly enhanced relaxation rates of nuclei close to the spin-label. The resulting reduction in signal intensity was estimated from the relative peak volumes in a [^{15}N,^{1}H]-HSQC spectra recorded before and after addition of the spin-label. Furthermore, the results from these experiments were compared to the results obtained for wild-type NPY (*15*) (Figure 6).

A nearly identical pattern of relative intensities for both peptides is found at the N-terminus up to residue 15. The 3−4 residue periodicity for the amount of reduction in signal intensity, which was also noticed in the case of NPY bound to DPC micelles and which is typical for helices associated parallel to the micelle surface, is observed in the segment 17−29. Local minima in signal intensity upon addition of 5-doxylstearate agree perfectly for residues 17, 21, 24/25, and 29. However, the signal intensity of Ile^{28} and Asn^{29} are very similarly affected in wild-type NPY, whereas in [Ala^{31}, Pro^{32}]-NPY the remaining signal intensity of Ile^{28} is 3 times larger than for Asn^{29} after addition of the spin-label. On the contrary, the signal of Leu^{30} is reduced to about the same extent as for Asn^{29} in wild-type NPY. These findings suggest that membrane anchoring is no longer mediated by Ile^{28}/Asn^{29} as observed in NPY but rather shifts to Asn^{29}/Leu^{30} in the mutant.

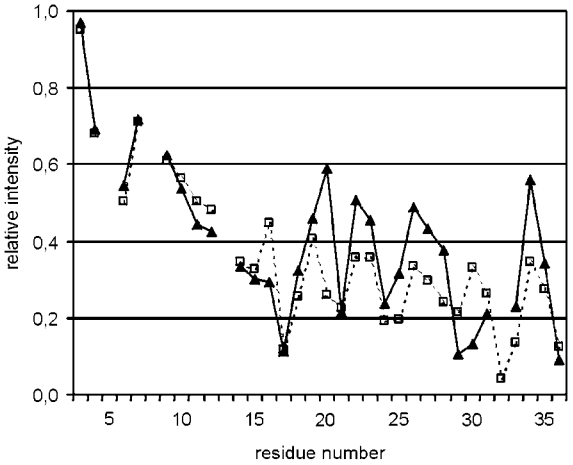

FIGURE 6: Comparison of the residual relative signal intensity in [^{15}N,^{1}H]-HSQC spectra between [Ala^{31}, Pro^{32}]-NPY (—▲—) and wild-type NPY (- -□- -) bound to DPC micelles upon addition of 5 mM of the spin-labeled 5-doxylstearic acid.

Conclusions drawn from the chemical shift differences and from NOE data support the view that the most dramatic perturbation of the conformation is localized around residues 29/30. Apparently, many signals of nuclei in the helical segment comprising residues 17−28 are reduced to a lesser extent in the mutant as compared to NPY. We therefore argue that the mean distance of these residues to the spin-label is larger due to a weaker membrane association. Alternatively, the orientation of [Ala^{31}, Pro^{32}]-NPY may be better defined on the membrane such that certain protons are fixed in a position opposite to the membrane surface further away from the spin-label for most of the time. The latter argument implies that wild-type NPY slightly wobbles about its helical axis when bound to the membrane. The weak reductions at the C-terminus, especially for Gln^{34}, might be attributed to the already proposed increased flexibility in that segment. However, it has to be emphasized that the Tyr^{36} amide belongs to the residues that are affected by the spin-label in both NPY and the Y_5-receptor-selective peptide to the largest extent. Thus, although the mutant is speculated to be more flexible between Arg^{33}−Tyr^{36}, the C-terminus cannot be considered to diffuse randomly in the aqueous environment but rather seems to be anchored onto the micelle surface.

Amide Proton H/D Exchange. By measuring the proton/deuterium exchange time-course for pNPY, we previously found that nearly all peaks in a 2D [^{15}N,^{1}H]-HSQC spectrum had vanished only 10 min after addition of D_2O to a lyophilized sample, except for the signals of residues Leu^{24}, Arg^{25}, Tyr^{27}, Ile^{28}, and Ile^{31}. Moreover, the signal of Ile^{28} was still strong after more than 70 min at 37 °C, indicating that the most persistent contacts between NPY and the membrane surface are mediated by residues in the C-terminal half of the helix (*15*). In [Ala^{31}, Pro^{32}]-NPY, only the four peaks of residues 21 (Tyr), 24, 25, and 28 are still visible after 10 min. Moreover, in the mutant the most efficient shielding from solvent access is now observed for residue Leu^{24}, which only disappears after 40 min of measurement. Obviously, the main association points with the membrane are shifted toward the N-terminal half of the helix in the mutant, whereas the lack of anchoring residues in positions 31 and 32 lead to a lower affinity of [Ala^{31}, Pro^{32}]-NPY to DPC micelles.

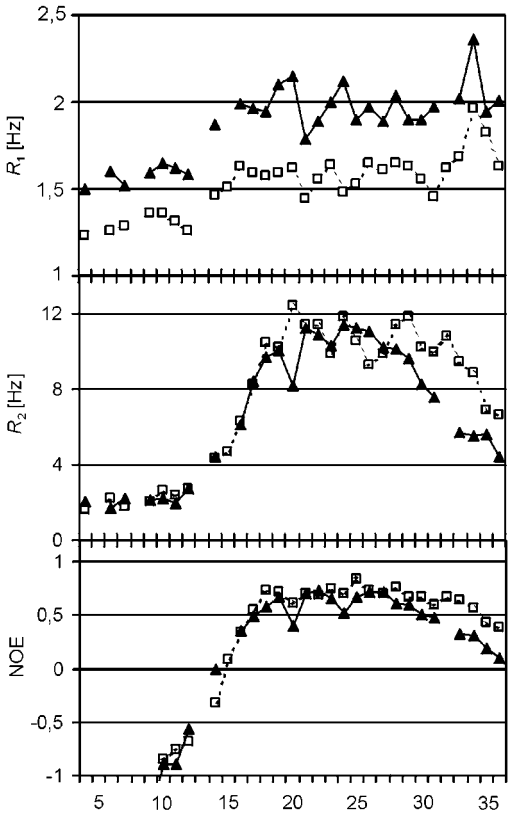

FIGURE 7: Comparison of the ^{15}N-relaxation rate constants R_1, R_2, and ^{15}N{^{1}H}-NOEs between [Ala^{31}, Pro^{32}]-NPY (—▲—) and wild-type NPY (- -□- -) bound to DPC micelles, determined at 500 MHz, versus the residue number.

Backbone Dynamics. To further characterize the [Ala^{31}, Pro^{32}]-NPY/DPC system, we have probed the dynamics of the molecule using ^{15}N-relaxation. The latter supplies information on the magnitude of motions of ^{1}H/^{15}N bond vectors in a coordinate system that is synchronized to overall tumbling. The present analysis is based on ^{15}N R_1 and R_2 relaxation rates recorded at both 500 and 600 MHz as well as ^{15}N{^{1}H}-NOE data at 500 MHz on a 1 mM uniformly ^{15}N-labeled [Ala^{31}, Pro^{32}]-NPY sample.

At 500 MHz, the average R_1 values for Lys^{4}−Ala^{14} and Asp^{16}−Tyr^{36} were 1.62 ± 0.11 and 1.99 ± 0.12 Hz, respectively. R_2 is 2.12 ± 0.31 Hz at Lys^{4}−Ala^{12}, is 4.44 Hz at Ala^{14}, and increases to 10.0 up to residue Arg^{19}. It is 9.98 ± 1.34 Hz at Tyr^{20}−Ile^{31} and drops to 5.29 ± 0.60 Hz at the C-terminal tetrapeptide. At Lys^{4}−Ala^{14}, the heteronuclear NOE, which very sensitively reflects changes in rigidity, is negative (in the range of −8.38 and 0), adopts values from 0.36 to 0.67 between Asp^{16} and Tyr^{20}, and is >0.6 for almost all residues between Tyr^{21}−Ile^{28} (0.67 ± 0.07). Toward the C-terminus, the value of the NOE steadily decreases from a value of 0.59 at Asn^{29} to 0.10 at Tyr^{36}. Because of problems in the peak volume integrations of residue 15, the corresponding relaxation rate constants could not be determined. The local fluctuations of the R_1 and R_2 data measured at 600 MHz are qualitatively very similar to the 500 MHz parameters (data not shown). As compared to wild-type NPY on DPC micelles, the R_1(500) are on average 22% (±8%) higher than those of the mutant, but the local fluctuations of the data are again very similar (Figure 7).

The R_2(500) rates are similar for both peptides within ±1 Hz at nearly all residues between Lys^{4}−Ile^{28}. However, in

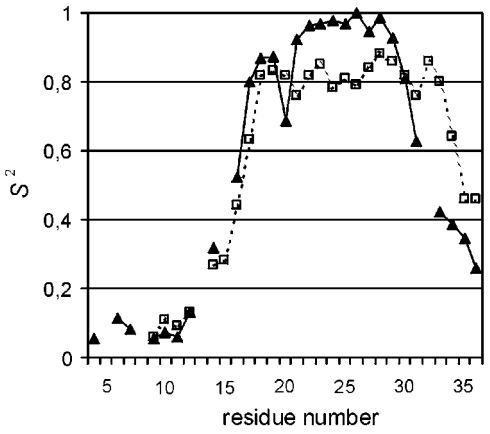

FIGURE 8: Comparison of the generalized order parameters S^2 between [Ala[31], Pro[32]]-NPY (—▲—) and wild-type NPY (- -□- -) bound to DPC micelles, as determined from ^{15}N-relaxation measurements.

the C-terminal segment comprising Asn[29]−Tyr[36], they are systematically lower in the mutant by 2−3.75 Hz, indicating increased flexibility for that part of the backbone. In accordance with the R_2 rates, systematically lowered NOEs (between −0.12 and −0.32) are found at the C-terminal hexapeptide Leu[30]−Tyr[36].

Similarly to our analysis for wild-type NPY bound to DPC micelles (*15*), we calculated the correlation time for overall tumbling, the generalized order parameters, and effective correlation times for internal motions on one or two different timescales according to the Model-Free approach (*47*−*49*). The first estimate of the overall (isotropic) rotational correlation time was obtained from the average value of R_2/R_1 nuclei for residues in the segment 21−29, for which the heteronuclear $NOE_{(500)}$ was larger than 0.6 (*63*). These are $(R_2/R_1)_{500} = 5.49$ (±0.48) and $(R_2/R_1)_{600} = 8.04$ (±0.90), corresponding to correlation times τ_c of 8.17 ± 0.43 and 8.48 ± 0.56, respectively. Fixing $\tau_c = 8.2$ ns, as estimated from the 500 MHz data, we selected the internal motional parameters S^2, S_f^2, S_s^2, t_e, and R_{ex}, respectively, according to the statistical approach initially described by Mandel et al. (*51*). Fitting to one of the proposed models was well possible for almost all residues, except Asp[11], Ala[12], Asp[16], and Asn[29], for which the sum-squared error residuals exceeded the 95% confidence interval of the χ^2-distribution slightly. However, replacement of the selected models by any of the more complex ones did not significantly improve the fits. Finally, the motions of residues Lys[4]−Asn[7] as well as Leu[17]−Leu[30] were described by the simple model-free formalism (SMF), whereas the extended model-free formalism (EMF) was applied for fitting the relaxation data of the helix-capping residues Gly[9]−Asp[16] and Ile[31]−Tyr[36]. A small chemical exchange contribution of 1.8 Hz had to be introduced at Leu[24]. A complete listing of the parameter from the fit is given in the Supporting Information.

After the final optimization, the overall rotational correlation time was at 8.22 (±0.09) ns, as compared to the value of 8.96 (±0.10) ns as determined for wild-type NPY bound to DPC micelles.

The values of the derived generalized order parameter are similar for the N-terminal residues up to Arg[19] (Figure 8). However, systematically higher values of S^2 are encountered in the segment of residues Tyr[21]−Asn[29] of the Y_5-receptor-selective mutant, in which the backbone is almost perfectly rigid ($S^2 = 0.96 \pm 0.03$), as compared to a mean order parameter of $S^2 = 0.82 \pm 0.04$ between Ala[18] and Arg[33] for wild-type NPY (*15*). On the contrary, corresponding S^2 values are between 0.11 and 0.38 lower for Ala[31]−Tyr[36] in the mutant than in wild-type NPY. Thus, the dipeptide [Ala[31], Pro[32]] increases the flexibility mostly at the location of its introduction, thereby confirming NOE and chemical shift data as well as coupling constants. On the other hand, the loss of rigidity of the mutant at the C-terminus is counterbalanced by increased stability of the central part of the helix. Again, we speculate, that this fact might be due to a better anchoring and a more well-defined orientation of [Ala[31], Pro[32]]-NPY on the membrane.

DISCUSSION

Interest in Y_1- and Y_5-receptor subtypes has recently been steered by the fact that they are supposed to mediate the orexigenic action of NPY (*7*) and therefore present interesting targets for the design of anti-obesity drugs. The newly developed class of Y_5-receptor-selective mutants (*1*, *64*, and Cabrele et al., companion paper), some of which could be shown to act as agonists, provide important tools to study the pharmacological role of this receptor subtype. Accordingly, [Ala[31], Aib[32]]-NPY has served to demonstrate the importance of the Y_5-receptor in the stimulation of food intake (*1*).

Of course, structure-based drug design would tremendously benefit from the knowledge of the peptide conformation in its receptor-bound form. However, the difficulties in expression, purification, and reconstitution of functional G-protein coupled receptors (GPCRs) have so far prevented direct structure determinations of ligand−GPCR complexes, either by NMR or X-ray crystallography. Recently, the conformation of the pituitary adenylate cyclase activating polypeptide mutant PACAP(1−21)-NH_2, bound to its GPCR, has been solved using 2D transferred nuclear Overhauser effect spectroscopy (*65*). In their investigation, Inooka et al. discovered that the C-terminal region comprising residues 8−21 forms an α helix. This structure is very similar to that of micelle-bound PACAP (RMSD < 1 Å). However, a β-coil element for residues 3−7 of the N-terminus exists only in the receptor-bound state, thereby producing a hydrophobic patch which is essential for receptor binding.

We believe that the observations on PACAP and our results presented in this work can be nicely explained within the framework of the message-address concept which was introduced by Schwyzer in his Membrane Compartments Theory (*20*, *66*). Accordingly, the amphipathic helical portion of PACAP and similarly of other peptide hormones serves as the address to target the molecule to the membrane surface. They do so by providing necessary contacts to the membrane through hydrophobic residues that intercalate into the lipid interior. These interactions stabilize the helix only in vicinity of a membrane such that otherwise unstructured peptides adopt a unique fold. The hormone then diffuses two-dimensionally laterally along the membrane surface in search of its receptor. Finally, receptor recognition and binding might go hand-in-hand with a conformational change (induced fit) at selected portions of the molecule (the so-called message) allowing for specific interactions between the

ligand and the receptor. Such a two-step ligand transportation model (*65*) is supposed to be entropically favorable, because only a few dihedral angles in the flexible part of the molecule become conformationally restricted upon receptor binding. Because of the mechanism that involves membrane association as a first step, moderate-to-high affinity of the hormone to the membrane is required. High-affinity binders display high on-rates and low off-rates for membrane binding. It has recently been emphasized that the two events are controlled by different mechanisms (see Selzer et al. (*67*) and references therein). High on-rates require far-reaching forces and are therefore promoted through favorable electrostatic forces. Low off-rates are most efficiently achieved through multiple hydrophobic contacts. In view of this concept, NPY as well as the mutant are optimized in both respects; the C-terminal helix comprises hydrophobic membrane−surface exposed residues as well as positively charged Arg residues. In close analogy to PACAP, the secondary structure of NPY can be characterized by a C-terminal α helix (residues Asp^{16}−Tyr^{36}) and a completely flexible N-terminus (*13*, *15*, *68*). Recently, we determined the structure, orientation and backbone dynamics of NPY on DPC micelles (*15*). We found that the presence of the phospholipid membrane stabilizes the α helix and induces a conformational change at the C-terminal tetrapeptide as compared to the unligated solution structure of NPY. In our view, Thr^{32} and Tyr^{36}−NH_2 anchor NPY on the membrane such that Arg^{33} and Arg^{35} are placed in the aqueous phase but still are positioned close to the membrane surface. In doing so, they are able to make contacts to the receptor as a part of the message (see the following discussion). Similarly, the central part of the amphiphilic helix (residues 16−31) serves as the address targeting and orientating NPY on the membrane surface, whereas the N-terminus is most probably another part of the message at some receptor subtypes.

In the presented class of NPY mutants (Cabrele et al., companion paper), selectivity in binding to the Y_5-receptor with retained affinity is achieved through introduction of the dipeptide [Ala^{31}, Xxx^{32}], with Xxx being either Aib, Pro, or Hyp just next to the C-terminal message sequence. To understand the selective recognition of these mutants by only one receptor subtype on a structural level, we focus our analysis in the following on differences between [Ala^{31}, Pro^{32}]-NPY and wild-type NPY with respect to their structure and dynamics in the presence of the membrane-mimicking dodecylphosphocholine micelles.

Summarizing our results, we find the following. (1) None of the measured data are indicative of significant differences with respect to structure or dynamics for the N-terminal residues 1−20 between NPY and the mutant. (2) Chemical shift data and $^3J_{HN\alpha}$ coupling constants as well as generalized order parameters determined from ^{15}N-relaxation parameters clearly demonstrate a rather rigid backbone between residues Tyr^{21}−Asn^{29} in the mutant, while NPY exhibits some residual flexibility. This observation might be due to the fact that more extended helices that are stably anchored to micelle surfaces need to become more flexible in order to accommodate for the surface bend and the fact that there is little long-range order of the lipid molecules. (3) We have identified a slightly altered membrane-anchoring mode in the mutant. The anchoring residues were recognized by their proximity to the membrane-integrating spin-label and displayed largest levels of signal reduction at residues 17, 21, 24, 29/30, and 36. Hence, the anchor at residues 28/29 in wild-type NPY is shifted to residues 29/30 in the mutant. Moreover, the absolute differences between minima and maxima were more pronounced than in wild-type NPY. We propose that the orientation of [Ala^{31}, Pro^{32}]-NPY with respect to the membrane surface may be very well-defined, whereas wild-type NPY slightly wobbles about its helical axis. Moreover, a proton/deuterium exchange experiment shows a faster overall exchange kinetics in the mutant. The most efficient shielding from the solvent is observed for the amide proton of Leu^{24} in the mutant. We therefore propose that the principal site-mediating membrane association is shifted from Ile^{28} in wild-type NPY to Leu^{24}/Tyr^{21} in the mutant, possibly due to the substitution of membrane-anchoring residues Ile^{31}−Thr^{32}. In combination with the significantly lower overall correlation time of [Ala^{31}, Pro^{32}]-NPY, we suggest a weaker membrane affinity constant for this type of NPY mutant. (4) Finally, we notice the lack of $H_\alpha N$ (*i*,*i*+*3)* NOEs between residues 26 and 29. Together with the fact that the membrane anchor is shifted by one position toward the C-terminus in this part, we propose a π-helical turn for the mutant at the end of the helix rather than an α helix. (5) As mentioned previously, the increased rigidity in the central helix of the mutant is compensated by a much more flexible C-terminal pentapeptide. The positions of the mutations present starting points after which the regular secondary structure is interrupted. This is evident from lowered order parameters, the lack of medium-range NOEs, and from secondary chemical shifts which are more close to the random coil values for [Ala^{31}, Pro^{32}]-NPY. However, Tyr^{36}−NH_2 is apparently again in close vicinity to the membrane, a fact that is obvious from the signal reductions for protons of this moiety observed in the spin-label experiment; hence, the C-terminus folds back onto the membrane surface. This interpretation is further supported by decreasing secondary chemical shift differences of H^N and $C_\alpha H$ protons between the mutant and NPY.

In the following, we would like to comment briefly on two points of interest. First, the more pronounced differences between minima and maxima of signal reductions in the spin-label experiment add further evidence for a more stable helix in the segment comprising residues Tyr^{21}−Asn^{29} in the mutant. Any residual flexibility will allow (membrane-averted) protons of the hydrophilic side of the helix to approach the spin-label more closely for some time. Because the effect of the spin-label depends on the 6th power of the distance, this will have a remarkable effect on the observed signal reductions and will level off the differences to some extent. Second, a contradiction seems to exist between the steady decrease of the generalized order parameter S^2 toward the C-terminus and the statement that the C-terminal Tyr^{36}−NH_2 group serves as a membrane anchor. However, we like to emphasize that the spin-label only probes the distance to the membrane surface. In accordance with both data, we propose that the C-terminal tetrapeptide segment diffuses freely in two dimensions along the membrane surface around its anchor point at residue 29/30. In doing so, the order parameter will decrease in the observed fashion but the membrane anchor will keep the last residue still close to the surface. In that context, it is of interest to notice that the order parameter decreases more slowly at the C-cap of

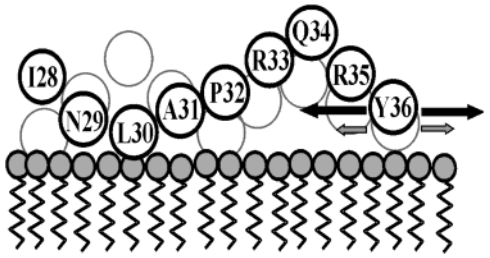

FIGURE 9: Model for the topological orientation of the C-terminal loop of [Ala^{31}, Pro^{32}]-NPY on the dodecylphosphocholine micelle surface. The corresponding spatial arrangements of residues of wild-type NPY are shown in gray for comparison.

the helix than at the N-cap, which can be explained by the additional terminal anchor. Finally, a change in the orientation (as is expected by introduction of D-Pro instead of Pro at position 32) abolishes any binding affinity for the Y_5-receptor. In an attempt to visualize these statements, we propose a model for the conformation at the C-terminus, as shown in Figure 9. To summarize, the pentapeptide Ala^{31}−Arg^{35} can be considered as a flexible loop being anchored to the membrane through residues Asn^{29}/Leu^{30} as well as through Tyr^{36}−NH_2.

In conclusion, we draw the following scenario of the events that finally lead to receptor recognition of NPY and subtype selective mutants. In a first step, the hydrophobic side of the amphiphilic helix of NPY binds to the membrane. Considering the fact that in the presence of DPC micelles only a single set of resonances is observed in the ^{15}N,^{1}H correlation map and that all NOE data can be fitted to a single structure without problems, we conclude that it is the membrane-bound form that predominates and makes the initial receptor contact. Moreover, removal of the hormone from the membrane is energetically unfavorable. First experimental evidence for neuropeptide Y-membrane interactions was obvious from NPY-induced leakage of carboxyfluorescein entrapped in liposomes, liposome binding measurements by centrifugal filtration, and differential scanning calorimetry using dimyristoylphosphatidylcholine (DMPC) micelles. On one hand, these studies clearly demonstrated that NPY and linear analogues of NPY interact with membranes. On the other hand, the cyclic analogue [D-Cys^2, 8-aminooctanoic acid$^{5-24}$, Cys^{27}]-NPY in which the N- and the C-terminal regions are constrained, still bound to pig spleen receptors in the submicromolar range while lipid binding was very ineffective (*69*, *70*). At least in this analogue, lipid binding does not contribute to the receptor binding energy. Minakata et al. (*71*) had designed five amphiphilic NPY models with multiple substitutions on the hydrophobic side of the helix between residues 13−32. From their data, they had demonstrated that the surfactant properties of NPY result from its potential to form amphiphilic secondary structures and not from specific amino acid sequences in this region. In one of the peptides, they changed three hydrophobic residues by leucines and three tyrosines by phenylalanines. Although this changed the conformation and self-association in solution, this peptide showed, nevertheless, 20% of the potency of NPY in inhibiting the electrically stimulated contractions of the rat vas deferens. Hence, the main role of the hydrophobic residues might be anchoring on the membrane rather than specific interactions with the receptor. We suggest that, upon binding to the membrane, some residues on the hydrophilic side are prepositioned so that receptor recognition is facilitated. These are for instance Arg^{33} or Arg^{35} that may not be substituted by alanine without dramatic or complete loss of activity at the Y-receptors (*72*−*74*). In the Y_5-receptor-selective mutants, these residues are exposed to the aqueous environment in a wider loop anchored by residues 29/30 and 36 on the membrane. In NPY, Arg^{33} and Arg^{35} are placed in the aqueous compartment as well but in a regular α-helical turn anchored to the membrane by residues 32 and 36. As a consequence, the basic residues are more flexible in the mutant, and their distance from the membrane−water interface is larger on average. One possible scenario during the initial contact with the receptor is that these charged residues form an electrostatic attraction with acidic residues from the receptor loops (e.g., a salt-bridge) that may very favorably contribute to the free energy of binding and hence increase the affinity to the receptor. Selzer et al. (*67*) succeeded in the design of faster associating protein complexes by incorporating charged residues in the vicinity of the binding interface, based on the fact that the rate of association can be increased by favorable electrostatic interactions. Similarly, we speculate that the presented class of NPY mutants is selectively attracted by the Y_5-receptor subtype because in that particular case spatial charge complementarity between the positively charged Arg residues from the ligands and negatively charged receptor residues may exist. Such a favorable electrostatic attraction due to an Arg−Asp interaction was observed by Giragossian and Mierke (*75*) in their structure of CCK-8 bound to the DPC-anchored third extracellular loop of the CCK receptor. Once NPY or the mutants have been guided into close vicinity of residues from the loop, other contacts in the receptor−ligand complex which triggers the intracellular signal may be formed via induced fit. To investigate whether the C-terminal loop itself is sufficient for selectivity, we have synthesized NPY(1−32), Ala, Pro,$^{33-36}$ NPY(33−36)-NH_2. However, binding affinity at the Y_5-receptor dropped by at least 1 order of magnitude, clearly demonstrating that other factors such as relative orientation of loop and helix residues, overall length of the binding domain, and so forth are of importance (Cabrele et al., companion paper). Moreover, we like to emphasize that our view is primarily important for the *initial* contact and that further data on the receptor−ligand complex are required. In addition, from the work by McLean (*69*, *70*, vide supra), it becomes obvious that not all ligands at the Y-receptors display the same mode of binding and, hence, that the membrane-bound conformation may only be of importance for a subset of ligands. Nevertheless, Inooka et al. (*65*) found that the membrane-bound conformation of the peptide PACAP is very similar to the conformation in the complex. A question arises whether structural features that might be important for receptor recognition in the membrane-bound state can already be detected in the unligated peptides (see companion paper). When comparing the solution structure of the Y_5-receptor-selective mutant [Ala^{31}, Aib^{32}]-NPY with the conformation of membrane-bound [Ala^{31}, Pro^{32}]-NPY, it becomes obvious that in both cases the α helix, which in NPY more or less extends up to the last residue, is interrupted through the introduced mutation. Hence, we suspect that gross-structural features of the membrane-bound form are already preformed in solution

such as the length and the position of the α helix. The 3_{10}-helix observed between residues 28 and 31 in the solution structure of [Ala[31], Aib[32]]-NPY indicates that the helix is destabilized toward the C-terminus. Moreover, the structural bundle is ill-defined from residue 31 onward in solution. Upon binding to the membrane, free diffusion of the C-terminal pentapeptide is restricted through the additional membrane-anchoring Tyr amide, thereby introducing a long and rather flexible loop. In that respect, although the conformation in solution and in the membrane-bound form contains differences that are important for binding such as the orientation of the C-terminus, other important features apparently already emerge in solution. Hence, screening of ligands by CD spectroscopy in solution may still be considered to be very useful to preselect peptides that will later on be structurally characterized in their membrane-bound state by NMR. Thereby, together with the accumulated knowledge stemming from previous structure−activity relationship within the NPY family multiligand/multireceptor system (*17*), the full potential of rapid solid-phase peptide synthesis may be combined with detailed structural characterization to develop more potent and more selective ligands.

ACKNOWLEDGMENT

We thank the group of Professor G. Folkers for lab space and interest in our work.

SUPPORTING INFORMATION AVAILABLE

Tables of chemical shifts, ^{15}N-relaxation parameters, backbone dynamical parameters, and structural information for [Ala[31], Pro[32]]-pNPY on DPC micelles. This material is available free of charge via the Internet at http://pubs.acs.org.

REFERENCES

1. Cabrele, C., Langer, M., Bader, R., Wieland, H. A., Doods, H. N., Zerbe, O., and Beck-Sickinger, A. G. (2000) *J. Biol. Chem. 275*, 36043−36048.
2. Tatemoto, K. (1982) *Proc. Natl. Acad. Sci. U.S.A. 79*, 5485−5489.
3. Dumont, Y., Martel, J. C., Fournier, A., St-Pierre, S., and Quirion, R. (1992) *Prog. Neurobiol. 38*, 125−167.
4. Michel, M. C., Beck-Sickinger, A., Cox, H., Doods, H. N., Herzog, H., Larhammar, D., Quirion, R., Schwartz, T., and Westfall, T. (1998) *Pharmacol. Rev. 50*, 143−150.
5. Gehlert, D. R. (1998) *Proc. Soc. Exp. Biol. Med. 218*, 7−22.
6. Stanley, B. G., and Leibowitz, S. F. (1985) *Proc. Natl. Acad. Sci. U.S.A. 82*, 3940−3943.
7. Gehlert, D. R. (1999) *Neuropeptides 33*, 329−338.
8. Criscione, L., Rigollier, P., Batzl-Hartmann, C., Rueger, H., Stricker-Krongrad, A., Wyss, P., Brunner, L., Whitebread, S., Yamaguchi, Y., Gerald, C., Heurich, R. O., Walker, M. W., Chiesi, M., Schilling, W., Hofbauer, K. G., and Levens, N. (1998) *J. Clin. Invest. 102*, 2136−2145.
9. Kanatani, A., Ito, J., Ishihara, A., Iwaasa, H., Fukuroda, T., Fukami, T., MacNeil, D. J., Van der Ploeg, L. H., and Ihara, M. (1998) *Regul. Pept. 75*−*76*, 409−415.
10. Rudolf, K., Eberlein, W., Engel, W., Wieland, H. A., Willim, K. D., Entzeroth, M., Wienen, W., Beck-Sickinger, A. G., and Doods, H. N. (1994) *Eur. J. Pharmacol. 271*, R11−R13.
11. Wieland, H. A., Engel, W., Eberlein, W., Rudolf, K., and Doods, H. N. (1998) *Br. J. Pharmacol. 125*, 549−555.
12. Darbon, H., Bernassau, J. M., Deleuze, C., Chenu, J., Roussel, A., and Cambillau, C. (1992) *Eur. J. Biochem. 209*, 765−771.
13. Monks, S. A., Karagianis, G., Howlett, G. J., and Norton, R. S. (1996) *J. Biomol. NMR 8*, 379−390.
14. Blundell, T. L., Pitts, J. E., Tickle, I. J., Wood, S. P., and Wu, C.-W. (1981) *Proc. Natl Acad. Sci. U.S.A. 78*, 4175−4179.
15. Bader, R., Bettio, A., Beck-Sickinger, A. G., and Zerbe, O. (2001) *J. Mol. Biol. 305*, 307−329.
16. Beck-Sickinger, A. G., and Jung, G. (1995) *Biopolymers 37*, 123−142.
17. Cabrele, C., and Beck-Sickinger, A. G. (2000) *J. Pept. Sci. 6*, 97−122.
18. Moroder, L., Romano, R., Guba, W., Mierke, D. F., Kessler, H., Delporte, C., Winand, J., and Christophe, J. (1993) *Biochemistry 32*, 13551−13559.
19. Sargent, D. F., and Schwyzer, R. (1986) *Proc. Natl Acad. Sci. U.S.A. 83*, 5774−5778.
20. Schwyzer, R. (1986) *Biochemistry 25*, 6335−6342.
21. Henry, G. D., and Sykes, B. D. (1994) *Methods Enzymol. 239*, 515−535.
22. Lauterwein, J., Bösch, C., Brown, L. R., and Wüthrich, K. (1979) *Biochim. Biophys. Acta 556*, 244−264.
23. Opella, S. J. (1997) *Nat. Struct. Biol. 4* (Suppl.) 845−848.
24. Opella, S. J., Kim, Y., and McDonnell, P. (1994) *Methods Enzymol. 239*, 536−560.
25. Brown, L. R., Bösch, C., and Wüthrich, K. (1981) *Biochim. Biophys. Acta 642*, 296−312.
26. Kosen, P. A. (1989) *Methods Enzymol. 177*, 86−121.
27. Kohno, T., Kusunoki, H., Sato, K., and Wakamatsu, K. (1998) *J. Biomol. NMR 12*, 109−121.
28. Weiner, M. P., Costa, G. L., Schoettlin, W., Cline, J., Mathur, E., and Bauer, J. C. (1994) *Gene 151*, 119−123.
29. Chen, Y. H., Yang, J. T., and Chau, K. H. (1974) *Biochemistry 13*, 3350−3359.
30. Live, D. H., Davis, D. G., Agosta, W. C., and Cowburn, D. (1984) *J. Am. Chem. Soc. 106*, 6104−6105.
31. Bartels, C., Xia, T.-h., Billeter, M., Güntert, P., and Wüthrich, K. (1995) *J. Biomol. NMR 6*, 1−10.
32. Griesinger, C., Otting, G., Wüthrich, K., and Ernst, R. R. (1988) *J. Am. Chem. Soc. 110*, 7870−7872.
33. Macura, S., and Ernst, R. R. (1980) *Mol. Phys. 41*, 95−117.
34. Kumar, A., Ernst, R. R., and Wüthrich, K. (1980) *Biochem. Biophys. Res. Commun. 95*, 1−6.
35. Otting, G. (1990) *J. Magn. Reson. 86*, 496−508.
36. Piotto, M., Saudek, V., and Sklenar, V. (1992) *J. Biomol. NMR 2*, 661−665.
37. Szyperski, T., Güntert, P., Otting, G., and Wüthrich, K. (1992) *J. Magn. Reson. 99*, 552−560.
38. Bodenhausen, G., and Ruben, D. J. (1980) *Chem. Phys. Lett. 69*, 185−189.
39. Palmer, A. G., III., Cavanagh, J., Wright, P. E., and Rance, M. (1991) *J. Magn. Reson. 93*, 151−170.
40. Kay, L. E., Keifer, P., and Saarinen, T. (1992) *J. Am. Chem. Soc. 114*, 10663−10665.
41. Grzesiek, S., and Bax, A. (1993) *J. Am. Chem. Soc. 115*, 12593−12594.
42. Güntert, P., Mumenthaler, C., and Wüthrich, K. (1997) *J. Mol. Biol. 273*, 283−298.
43. Weiner, P. K., Kollman, P. A., Nguyen, D. T., and Case, D. A. (1986) *J. Comput. Chem. 7*, 230−252.
44. Luginbühl, P., Güntert, P., Billeter, M., and Wüthrich, K. (1996) *J. Biomol. NMR 8*, 136−146.
45. Laskowski, R. A., Rullmannn, J. A., MacArthur, M. W., Kaptein, R., and Thornton, J. M. (1996) *J. Biomol. NMR 8*, 477−486.
46. Koradi, R., Billeter, M., and Wüthrich, K. (1996) *J. Mol. Graph 14* (51-5), 29−32.
47. Lipari, G., and Szabo, A. (1982) *J. Am. Chem. Soc. 104*, 4546−4559.
48. Lipari, G., and Szabo, A. (1982) *J. Am. Chem. Soc. 104*, 4559−4570.
49. Clore, G. M., Driscoll, P. C., Wingfield, P. T., and Gronenborn, A. M. (1990) *Biochemistry 29*, 7387−7401.
50. Palmer, A. G., III., Rance, M., and Wright, P. E. (1991) *J. Am. Chem. Soc. 113*, 4371−4380.
51. Mandel, A. M., Akke, M., and Palmer, A. G., III. (1995) *J. Mol. Biol. 246*, 144−163.
52. Schwyzer, R. (1987) *Embo J. 6*, 2255−2259.
53. Pellegrini, M., and Mierke, D. F. (1999) *Biopolymers 51*, 208−220.
54. Pellegrini, M., and Mierke, D. F. (1999) *Biochemistry 38*, 14775−14783.
55. Wüthrich, K. (1986) *NMR of Proteins and Nucleic Acids*, Wiley, New York.
56. Wishart, D. S., Sykes, B. D., and Richards, F. M. (1991) *J. Mol. Biol. 222*, 311−333.
57. deDios, A. C. (1996) *Prog. Nucl. Magn. Reson. Spectrosc. 29*, 229−278.

58. Wishart, D. S., Sykes, B. D., and Richards, F. M. (1992) *Biochemistry 31*, 1647−1651.
59. Zhou, N. E., Zhu, B.-Y., Sykes, B. D., and Hodges, R. S. (1992) *J. Am. Chem. Soc. 114*, 4320−4326.
60. Kuntz, I. D., Kosen, P. A., and Craig, E. C. (1991) *J. Am. Chem. Soc. 113*, 1406−1408.
61. Karplus, M. (1963) *J. Am. Chem. Soc. 85*, 2870−2871.
62. Wang, A., and Bax, A. (1996) *J. Am. Chem. Soc. 118*, 2483−2494.
63. Kay, L. E., Torchia, D. A., and Bax, A. (1989) *Biochemistry 28*, 8972−8979.
64. Cabrele, C., Wieland, H. A., Langer, M., Stidsen, C., and Beck-Sickinger, A. G. (2001) *Peptides 22*, 365−378.
65. Inooka, H., Ohtaki, T., Kitahara, O., Ikegami, T., Endo, S., Kitada, C., Ogi, K., Onda, H., Fujino, M., and Shirakawa, M. (2001) *Nat. Struct. Biol. 8*, 161−165.
66. Schwyzer, R. (1995) *Biopolymers 37*, 5−16.
67. Selzer, T., Albeck, S., and Schreiber, G. (2000) *Nat. Struct. Biol. 7*, 537−541.
68. Cowley, D. J., Hoflack, J. M., Pelton, J. T., and Saudek, V. (1992) *Eur. J. Biochem. 205*, 1099−1106.
69. McLean, L. R., Baron, B. M., Buck, S. H., and Krstenansky, J. L. (1990) *Biochim. Biophys. Acta 1024*, 1−4.
70. McLean, L. R., Buck, S. H., and Krstenansky, J. L. (1990) *Biochemistry 29*, 2016−2022.
71. Minakata, H., Taylor, J. W., Walker, M. W., Miller, R. J., and Kaiser, E. T. (1989) *J. Biol. Chem. 264*, 7907−7913.
72. Beck-Sickinger, A. G., Wieland, H. A., Wittneben, H., Willim, K. D., Rudolf, K., and Jung, G. (1994) *Eur. J. Biochem. 225*, 947−958.
73. McCrea, K., Wisialowski, T., Cabrele, C., Church, B., Beck-Sickinger, A. G., Kraegen, E., and Herzog, H. (2000) *Regul. Pept. 87*, 47−58.
74. Eckard, C. P., Cabrele, C., Wieland, H. A., and Beck-Sickinger, A. G. (2001) *Molecules*, in press.
75. Giragossian, C., and Mierke, D. F. (2001) *Biochemistry 40*, 3804−3809.
76. Braun, D., Wider, G., and Wüthrich, K. (1994) *J. Am. Chem. Soc. 116*, 8466−8469.

BI0201419